Electronic Supplementary Material (ESI) for CrystEngComm.

Supplementary Information

Polymorph Induced Diversity of Photomechanical motions of Molecular Crystals

Lei Gao, [a] Yunhui Hao, [a] Xiunan Zhang, [a] Xin Huang, [a] Ting Wang, *[a] and Hongxun Hao *[a]

[a] National Engineering Research Center of Industrial Crystallization Technology, School of Chemical Engineering and Technology, Tianjin University, Tianjin, 300072, P R China

Contents

Synthesis of *trans*-4AP

4-aminopyridine were purchased from Saen Chemical Technology Co., Ltd. Sodium hypochlorite (NaOCl), acetonitrile (CH_3CN) and ethyl acetate ($CH_3COOC_2H_5$) were purchased from Tianjin Jiangtian Chemical Co., Ltd.

Trans-4AP was synthesized by oxidative coupling of 4-aminopyridine by hypochlorite as reported previously.[1] A solution of 4-aminopyridine (5.0 g) was dissolved in 100 mL of water and then was added dropwise to 300 mL 0% NaOCl solution at 0 °C and stirred for 30 minutes. Then the orange precipitate was filtered and dried at 55 °C in vacuum oven for 24 hours. The crude product was purified by chromatography on silica gel (Acetonitrile: ethyl acetate=1:3) followed by rotary evaporation to remove solvent. The ^{1}H NMR spectrum is shown in Figure S1. The characteristic peaks of **δ** = 8.80 ppm and **δ** = 7.67 ppm on the ^{1}H NMR spectrum correspond to the hydrogen atoms with different environment on *trans*-4AP; the characteristic peak of **δ** = 7.25 ppm belongs to $CDCl_3$.

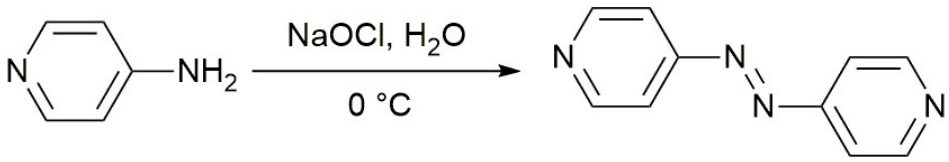

Scheme S1. Synthesis of *trans*-4,4'-azopyridine.

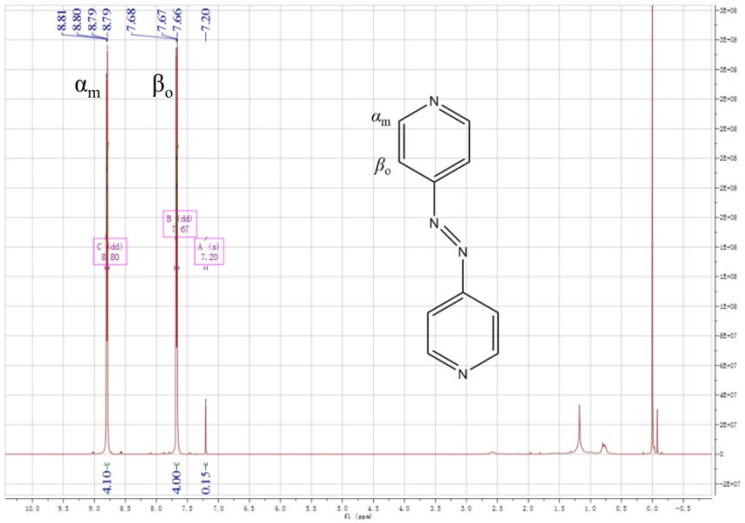

Fig. S1 ^{1}H NMR spectrum of *trans*-4,4'-azopyridine (400 MHz, $CDCl_3$, 25 °C, TMS): δ 8.80 (dd, J = 4.7, 1.4 Hz, 28H), 7.67 (dd, J = 4.7, 1.5 Hz, 27H).

Variable-temperature powder X-ray diffraction experiment

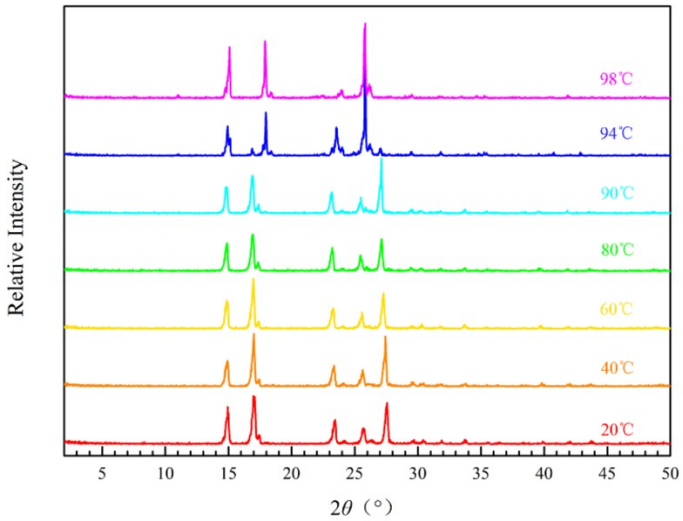

Fig. S2 PXRD patterns of *trans*-4AP crystals varied with temperature between 25 and 100 °C at a rate of 5 °C/min. The phase transition started at 92 °C and finished at 98 °C.

Molecule packing of Form 1 and Form 2 of *trans*-4AP crystal

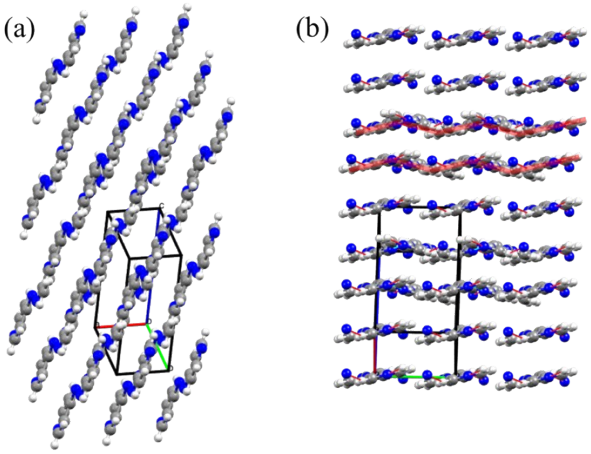

Fig. S3 (a) Flat molecular plane in Form 1 and (b) crinkled molecular plane in Form 2 of *trans*-4AP crystal.

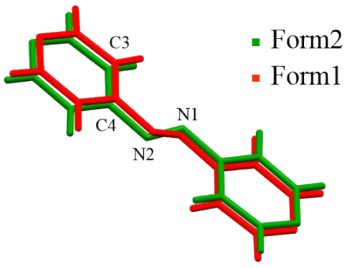

Fig. S4 Overlay diagrams between the different molecules in Form 1 and Form 2. The torsion angle between N1-N2-C4-C3 can be seen in Table S1.

Table S1. Torsions of individual molecules present in the two forms of *trans*-4AP.

Form	Torsion	Angle (°)
I	N1-N2-C4-C3	17.7
II	N1-N2-C4-C3	7.9

Table S2. Crystallographic data of different polymorph of *trans*-4AP.

cell parameters	Form2
Chemical formula	C_{10} H_8 N_4
Formula weight	184.20
Crystal system	monoclinic
Space group	P 2_1/n
Unit cell dimensions	*a* =4.7844 (10) [Å] α=90°
	b =6.1705 (12) [Å] *β*=96.42 (3)°
	c =15.430 (3) [Å] γ=90°
Z, Volume [Å^3]	2, 452.67 (16)
Temperature [K]	113 (2)
Limiting indices	-6<=h<=6, -8<=k<=8, -20<=l<=19
Reflections collected / unique	4568 / 1080 [R (int)] = 0.0461
Theta range for data collection [°]	2.657-27.919
Wavelength [Å]	0.71073
Calculated density [g cm^{-3}]	1.351
F [000]	192.0
Absorption coefficient [mm^{-1}]	0.088
Completeness to theta = 25.01°	99.9%
Max. and min. transmission	1 and 0.7654
Data / restrains / parameters	1080 / 0 / 64
R indices (all data)	R1 = 0.0547, wR2=0.1246
Final R indices [I > 2sigma(I)]	R1= 0.0447, wR2=0.1185
Goodness-of-fit on F^2	1.050

Analysis of crystal structure by Hirshfeld Surface and energy framework

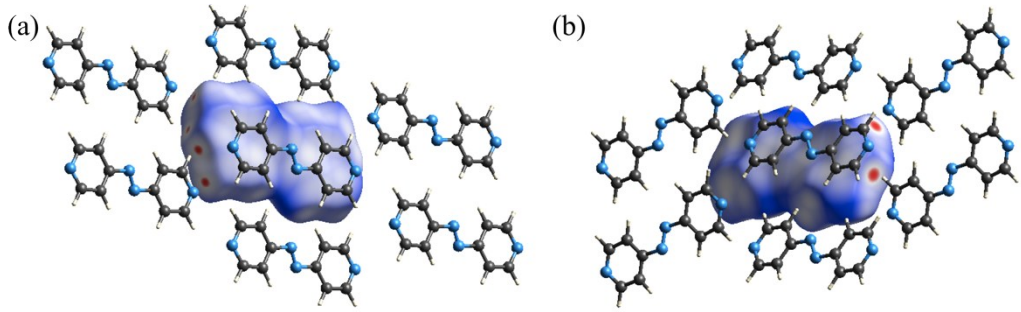

Fig. S5 Hirshfeld Surface of individual molecule in (a) Form 1 and (b) Form 2 of *trans*-4AP.

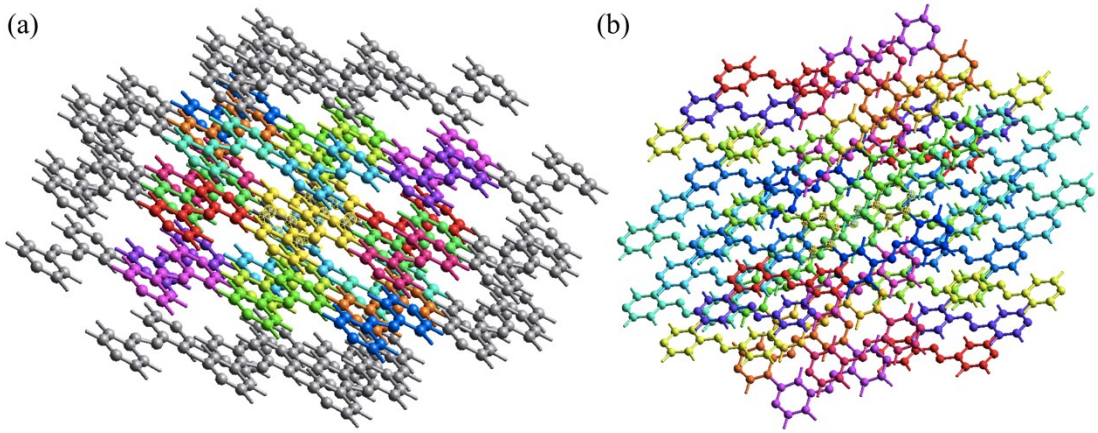

Fig. S6 Colour coding for the neighboring molecules around *trans*-4AP in (a) Form 1 (b) Form 2.

The value of interaction energies between neighboring molecules can be seen in Table S3 and S4.

Table S3. Interaction energies (kJ/mol) obtained from energy framework calculation for Form 1.

Interaction Energies (kJ/mol)
R is the distance between molecular centroids (mean atomic position) in Å.

Total energies, only reported for two benchmarked energy models, are the sum of the four energy components, scaled appropriately (see the scale factor table below)

	N	Symop	R	Electron Density	E_ele	E_pol	E_dis	E_rep	E_tot
	2	x, y, z	11.85	B3LYP/6-31G(d,p)	-12.9	-2.7	-9.3	13.2	-15.5
	2	x, y, z	6.45	B3LYP/6-31G(d,p)	2.2	-0.9	-13.7	6.7	-6.1
	2	x, y, z	10.32	B3LYP/6-31G(d,p)	-2.5	-1.0	-9.8	6.6	-7.9
	2	x, y, z	3.78	B3LYP/6-31G(d,p)	-1.5	-0.8	-51.8	27.7	-30.2
	2	x, y, z	11.31	B3LYP/6-31G(d,p)	-12.9	-2.5	-10.1	14.3	-15.4
	2	x, y, z	5.87	B3LYP/6-31G(d,p)	-6.2	-1.0	-23.1	14.8	-18.4
	2	x, y, z	11.84	B3LYP/6-31G(d,p)	-1.1	-0.1	-1.4	0.0	-2.4
	2	x, y, z	10.65	B3LYP/6-31G(d,p)	0.1	-0.0	-1.0	0.0	-0.7
	2	x, y, z	12.48	B3LYP/6-31G(d,p)	-0.2	-0.0	-0.3	0.0	-0.5
	0	x, y, z	12.46	B3LYP/6-31G(d,p)	-0.1	-0.0	-0.1	0.0	-0.2
	2	x, y, z	7.47	B3LYP/6-31G(d,p)	0.0	-0.0	-2.4	0.0	-2.1
	2	x, y, z	13.01	B3LYP/6-31G(d,p)	0.5	-0.2	-1.3	0.0	-0.8
	2	x, y, z	11.88	B3LYP/6-31G(d,p)	-0.3	-0.0	-0.3	0.0	-0.6

Scale factors for benchmarked energy models
See Mackenzie et al. IUCrJ (2017)

Energy Model	k_ele	k_pol	k_disp	k_rep
CE-HF ... HF/3-21G electron densities	1.019	0.651	0.901	0.811
CE-B3LYP ... B3LYP/6-31G(d,p) electron densities	1.057	0.740	0.871	0.618

Table S4. Interaction energies (kJ/mol) obtained from energy framework calculation for Form 2.

Interaction Energies (kJ/mol)
R is the distance between molecular centroids (mean atomic position) in Å.

Total energies, only reported for two benchmarked energy models, are the sum of the four energy components, scaled appropriately (see the scale factor table below)

	N	Symop	R	Electron Density	E_ele	E_pol	E_dis	E_rep	E_tot
	4	-x+1/2, y+1/2, -z+1/2	12.12	B3LYP/6-31G(d,p)	-0.0	-0.0	-0.2	0.0	-0.2
	2	x, y, z	11.39	B3LYP/6-31G(d,p)	-0.5	-0.0	-0.6	0.0	-1.1
	2	x, y, z	7.81	B3LYP/6-31G(d,p)	-1.8	-0.5	-11.0	7.1	-7.5
	4	-x+1/2, y+1/2, -z+1/2	14.46	B3LYP/6-31G(d,p)	-0.2	-0.0	-0.1	0.0	-0.3
	4	-x+1/2, y+1/2, -z+1/2	8.40	B3LYP/6-31G(d,p)	0.2	-0.0	-1.3	0.0	-1.0
	2	x, y, z	9.57	B3LYP/6-31G(d,p)	0.1	-0.0	-1.1	0.0	-0.9
	2	x, y, z	4.78	B3LYP/6-31G(d,p)	-1.5	-1.0	-44.7	23.4	-26.9
	4	-x+1/2, y+1/2, -z+1/2	15.26	B3LYP/6-31G(d,p)	0.2	-0.0	-0.2	0.0	0.0
	4	-x+1/2, y+1/2, -z+1/2	11.53	B3LYP/6-31G(d,p)	-10.8	-2.5	-8.3	12.1	-13.0
	4	-x+1/2, y+1/2, -z+1/2	8.88	B3LYP/6-31G(d,p)	-2.8	-0.6	-13.0	7.3	-10.2
	2	x, y, z	7.81	B3LYP/6-31G(d,p)	-0.4	-0.0	-1.8	0.0	-2.0
	4	-x+1/2, y+1/2, -z+1/2	12.45	B3LYP/6-31G(d,p)	-0.1	-0.0	-0.3	0.0	-0.4
	2	x, y, z	13.24	B3LYP/6-31G(d,p)	0.2	-0.0	-0.1	0.0	0.1
	2	x, y, z	6.17	B3LYP/6-31G(d,p)	-1.7	-1.1	-19.6	12.0	-12.3
	2	x, y, z	12.34	B3LYP/6-31G(d,p)	0.2	-0.0	-0.1	0.0	0.1

Scale factors for benchmarked energy models
See Mackenzie et al. IUCrJ (2017)

Energy Model	k_ele	k_pol	k_disp	k_rep
CE-HF ... HF/3-21G electron densities	1.019	0.651	0.901	0.811
CE-B3LYP ... B3LYP/6-31G(d,p) electron densities	1.057	0.740	0.871	0.618

Photoresponse of *trans*-4,4'-azopyridine molecules in liquid

The *trans*-4AP was dissolved in cyclohexane to explore the photoisomerization ability of *trans*-4AP molecule in liquid. UV-Vis absorption spectroscopy spectra of microcrystals were carried out on a UV-3010 spectrophotometer (HITACHI, Japan). The maximum UV absorption peak of *trans*-4AP molecule in cyclohexane was located at 287 nm. After irradiated with UV light (365 nm, 1200 mW cm^{-2}) for 5 min, the solution reached a photostationary state, and the maximum absorption peak intensity decreased by 3.3%. The photoisomerization can be further confirmed in ^{1}H NMR spectra which was collected in chloroform-d ($CDCl_3$) solution. After UV irradiation for 5 min, two new peaks appeared ^{1}H NMR spectrum in which were located in δ = 8.47 ppm and δ = 6.61 ppm. These two peaks correspond to the hydrogen atom on the *cis*-4AP molecule,[2] indicating that the *trans*-4AP molecule in the solution had undergone a *trans-cis* isomerization under UV light and transformed to *cis*-4AP. The decrease in the intensity of the maximum absorption peak in the UV spectrum was

also due to the decrease in *trans*-isomers. However, due to the effect of pyridine ring electron-withdrawing, the lifetime of the *cis*-isomer was short, and the equilibrium conversion of the *trans*-*cis* isomerization reaction was low and the estimated ratio of E/Z was about 98:2 in the PSS. Only a small part of the *trans*-isomers can be converted into the *cis*-isomers. The absorption peak intensity decreased in a small degree.

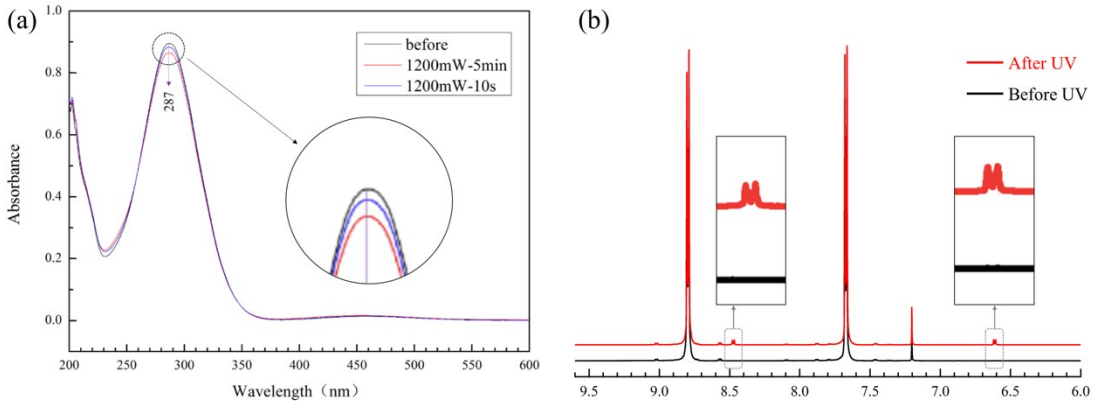

Fig. S7 (a) Absorption spectral change of *trans*-4AP (0.02mM) in cyclohexane; (b) ^{1}H NMR spectrum change of *trans*-4AP in $CDCl_3$.

Face indexing of *trans*-4AP crystal

The major face of Form 1 crystal was determined by SCXRD, as shown in Fig. S8 (a). The equilibrium morphology of *trans*-4AP under vacuum was calculated based on AE model in Materials Studio software.[3] The molecular geometry was firstly optimized in Dreiding and Universal force field for Form 1 and Form 2 respectively, and then the cell parameters were obtained. The morphology calculations were performed in Morphology module.

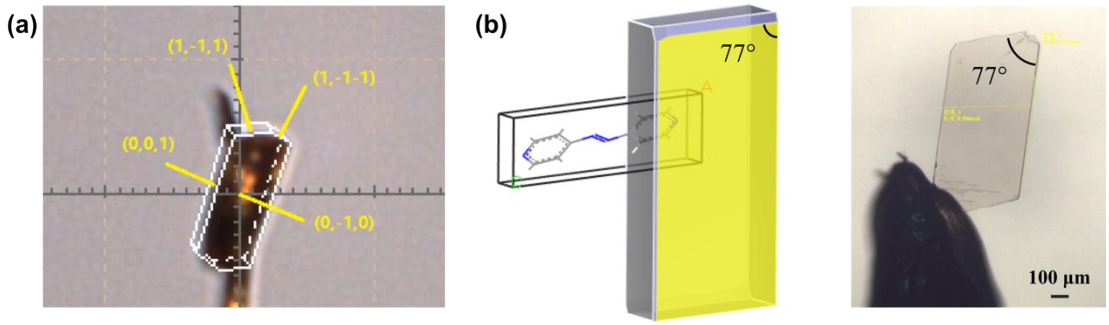

Fig. S8 (a) Face indexing of Form 1 crystal of *trans*-4AP. (b) Morphology of Form 1 crystal of *trans*-4AP. The major face is (010) Miller plane with parallelogram shape. The angle between the long and short sides is 77°， which is consistent with the actual shape of Form 1 crystal.

The dominant surface of Form 2 crystal was assigned by PXRD and predicted morphology. The plate-like crystals of Form 2 without grinding were placed flat on PXRD sample stage so that the strongest peak in the PXRD pattern corresponded to the most plane in the crystals, which is the

major face. Then the plate-crystals were grinded to take another PXRD test. These two patterns were compared to identify the major face. As can be seen in Fig. S10 (a), the strongest peak of unground crystals is at 14.84°, corresponding to (011) Miller plane. The predicted morphology of (011) Miller plane is in agreement with actual shape of Form 2 crystal. These results suggest that the dominant surface of Form 2 crystal is (011) face.

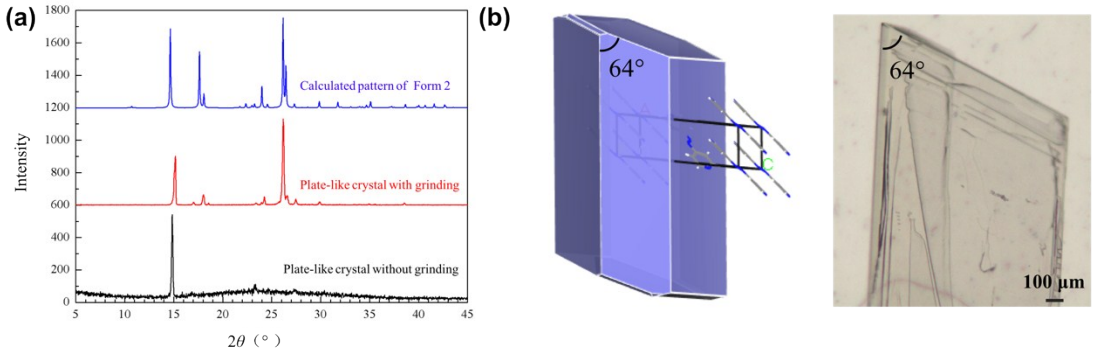

Fig. S9 (a) The PXRD pattern of Form 2 crystal without grinding. (b) The predicted morphology of Form 2 crystal of *trans*-4AP. The major face is (011) Miller plane with parallelogram shape. The angle between the long and short sides is 64°， which is consistent with the actual shape of Form 2 crystal.

Photomechanical motions of *trans*-4AP crystals

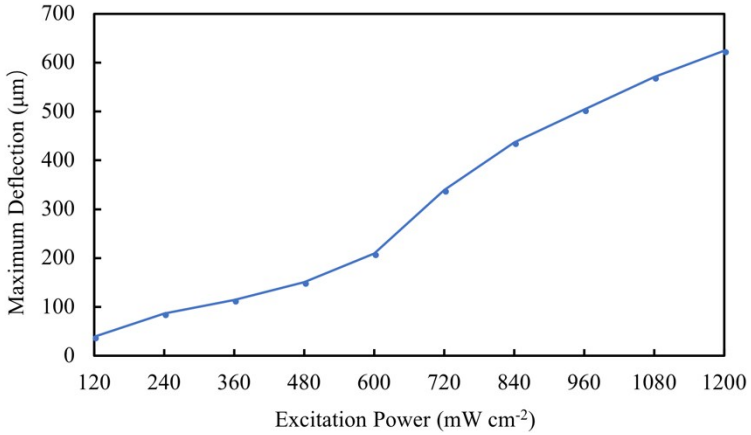

Fig. S10 Maximum deflection of narrow crystal of *trans*-4AP Form 2 on different UV excitation power. It increased with the increasing power.

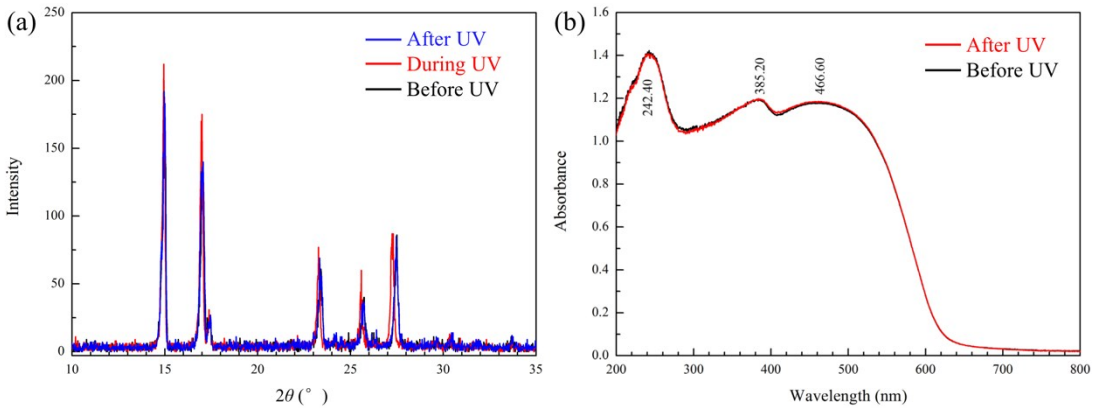

Fig. S11 (a) XRD pattern and (b) solid UV diffuse reflection spectrum change under UV irradiation of Form 1.

Table S5. Summary of the PXRD pattern change during UV irradiation of Form 1.

plane		2-Theta(deg)	d(Å)	Height	Area	FWHM
(010)	Before	14.982	5.9086	168	1857	0.188
	UV	14.941	5.9244	209	1990	0.162
	After	14.963	5.916	189	1948	0.175
(01-1)	Before	17.001	5.2111	129	1695	0.223
	UV	16.997	5.2123	171	1769	0.176
	After	17.058	5.1936	137	1927	0.239
(-100)	Before	23.400	3.7984	57	724	0.216
	UV	23.280	3.8178	72	617	0.146
	After	23.359	3.8051	52	713	0.233
(1-10)	Before	25.733	3.4591	34	303	0.152
	UV	25.579	3.4796	56	471	0.143
	After	25.682	3.4658	31	340	0.186
(1-11)	Before	27.498	3.241	81	810	0.17
	UV	27.240	3.2711	83	960	0.197
	After	27.461	3.2453	80	848	0.18

Table S6. Summary of the PXRD pattern change during UV irradiation of Form 2.

plane		2-Theta(deg)	d(Å)	Height	Area	FWHM
(011)	Before	15.057	5.8792	6240	30779	0.084
	UV	15.020	5.8934	2573	14547	0.096
	After	15.024	5.8919	2910	16246	0.095
(012)	Before	18.139	4.8866	208	2710	0.230
	UV	18.123	4.8909	160	1923	0.204
	After	18.119	4.8919	200	2486	0.203
(103)	Before	26.082	3.4136	159	2472	0.264
	UV	26.023	3.4212	133	2227	0.285
	After	26.098	3.4116	147	2306	0.267
(014)	Before	26.583	3.3505	211	2148	0.173
	UV	26.543	3.3553	167	1484	0.151
	After	26.562	3.3530	202	1578	0.133
(113)	Before	30.543	2.9245	206	985	0.081
	UV	30.501	2.9283	46	298	0.110
	After	30.517	2.9269	66	396	0.102

The crystal temperature was tested by a Tokia-Hit thermo plate system with thermocouple thermometer. The crystal was irradiated by different power UV light for 1 min and the temperature was recorded by the thermometer. When the temperature was cooled down to ambient temperature and stable, the next temperature point measurement is started.

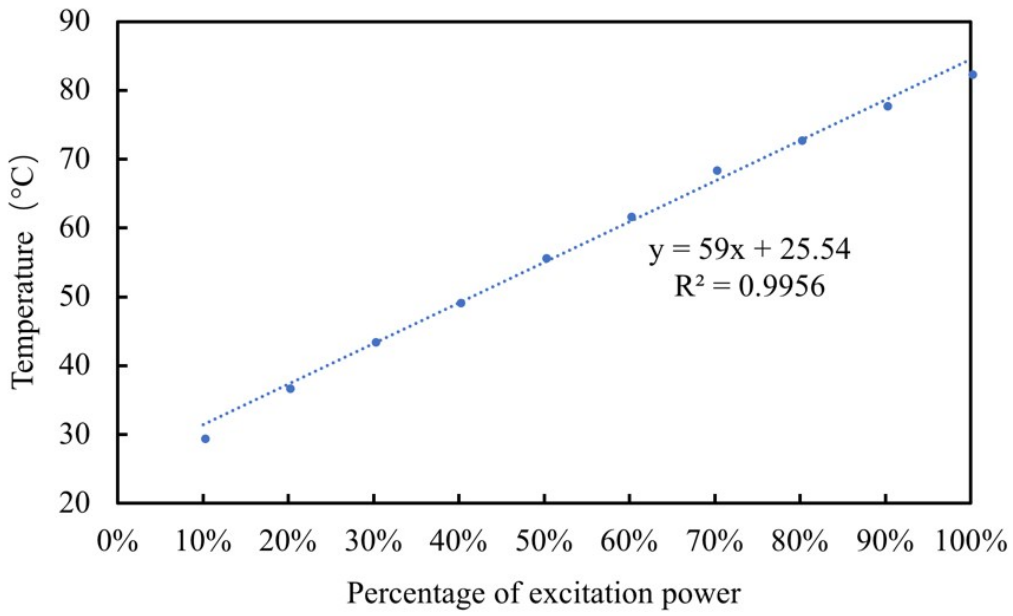

Fig. S12 Temperature change of *trans*-4AP crystal under UV light with increasing excitation power. The maximum of excitation power is 1200 mW cm^{-2}.

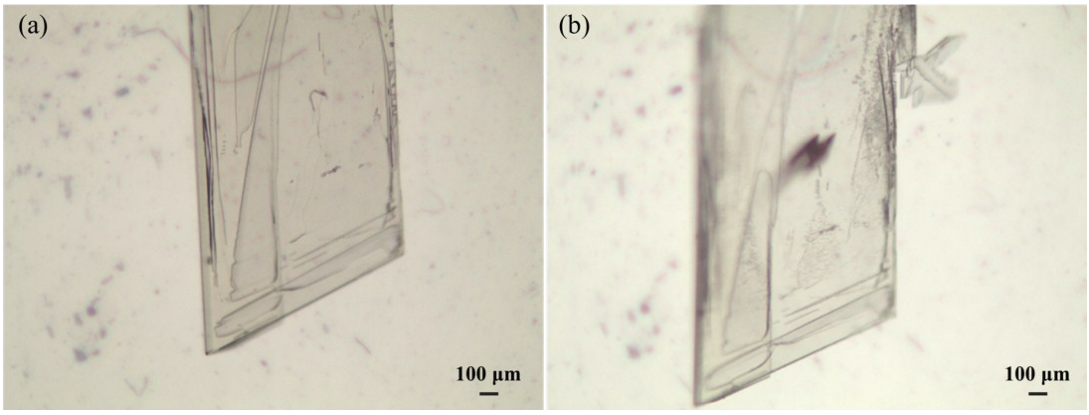

Fig. S13 Polarized light microscope picture of the *trans*-4AP crystal (a) before and (b) after irradiated for 20 minutes. The small black solids on the edge of crystal were recrystallized crystals.

Computer simulation of *cis*-4AP and *trans*-4AP molecule

The *cis*-4AP structure was optimized by Gaussian software using m062x/6-311G(d) level. The size of molecule was obtained via Multiwfn software.[4]

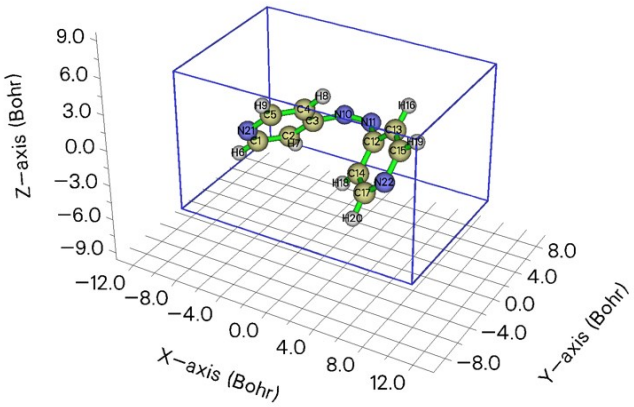

Fig. S14 Schematic diagram of *cis*-4AP molecular structure with the length of the three sides 10.435, 6.721, 6.239 Å, respectively.

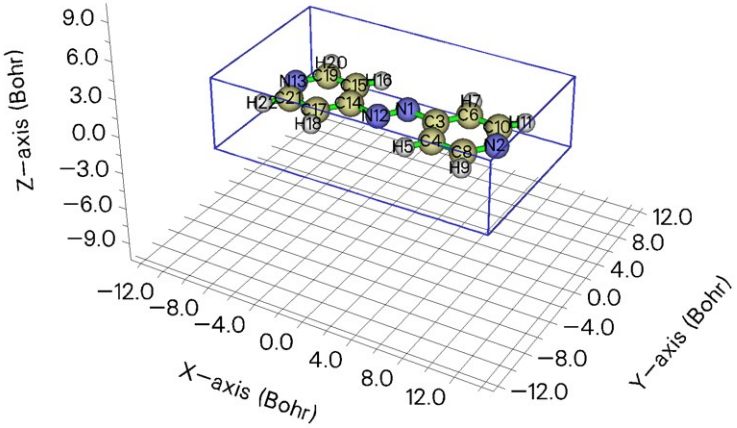

Fig. S15 Schematic diagram of *trans*-4AP molecular structure with the length of the three sides 11.815, 6.962, 3.100 Å, respectively.

Supporting moives

Movie 1. Photo-bending motion of Form 1 when irradiated with (0-10) face.

Movie 2. Photo-bending motion of Form 1 when irradiated with (010) face.

Movie 3. Backward photo-bending motion of Form 2 when irradiated with (011) face.

Movie 4. Forward photo-bending motion of Form 2 when irradiated with (0-1-1) face.

Movie 5. Photo-twisting motion of Form 2 when irradiated with (011) face.

Reference

1 G.-F. Liu, W. Ji and C.-L. Feng, *Langmuir*, 2015, **31**, 7122–7128.

2 E. V. Brown and G. R. Granneman, *J. Am. Chem. Soc.*, 1975, **97**, 621–627.

3 C. Wang, X. Zhang, W. Du, Y. Huang, M. Guo, Y. Li, Z. Zhang, B. Hou and Q. Yin, *CrystEngComm*, 2016, **18**, 9085–9094.

4 T. Lu and F. Chen, *J. Comput. Chem.*, 2012, **33**, 580–592.